Stochastic-Geometry-Based Analysis of Multipurpose UAVs for Package and Data Delivery

Yujie Qin, Mustafa A. Kishk, *Member, IEEE*, and Mohamed-Slim Alouini, *Fellow, IEEE*

***Abstract*—Using drones for communications and transportation is drawing great attention in many practical scenarios, such as package delivery and providing additional wireless coverage. However, the increasing demand for unmanned aerial vehicles (UAVs) from industry and academia will cause aerial traffic conflicts in the future. This, in turn, motivates the idea of this article: multipurpose UAVs, acting as aerial wireless data relays and means of aerial transportation simultaneously, to deliver packages and data at the same time. This article aims to analyze the feasibility of using drones to collect and deliver data from the Internet of Things (IoT) devices to terrestrial base stations (TBSs) while delivering packages from warehouses to residential areas. We propose an algorithm to optimize the trajectory of UAVs to maximize the size of collected/delivered data while minimizing the total round trip time subject to the limited onboard battery of UAVs. Specifically, we use tools from stochastic geometry to model the locations of the IoT clusters and the TBSs and study the system performance with respect to energy efficiency, average size of collected/delivered data, and package delivery time. Our numerical results reveal that multifunctional UAVs have great potential to enhance the efficiency of both communication and transportation networks.**

***Index Terms*—Data collection, Internet of Things (IoT) devices, multipurpose unmanned aerial vehicle (UAV), package delivery, Poisson point process, stochastic geometry.**

I. Introduction

WITH technological progress, unmanned aerial vehicles (UAVs, also known as drones) have recently drawn increasing interest from both industry and academia and are expected to play an essential role in potentially enhancing the performance of the next-generation wireless networks [1], [2], [3], [4], [5]. Unlike the traditional terrestrial base stations (TBSs), UAVs are more flexible and can easily satisfy the dynamic traffic demands by optimizing their locations in real time. Since they can adjust their altitudes, they are more likely to establish Line-of-Sight (LoS) links with ground users [6], [7]. At places where the users exhibit a certain degree of spatial clustering, and the density of active users varies with time, UAVs can rapidly function as aerial base stations (ABSs) and offer an additional dynamic capacity.

In addition, for the Internet of Things (IoT) devices specifically, UAV-evolved networks are more suitable. On the one hand, the transmit power of IoT devices is much lower compared to mobile users owing to their limited energy. Hence, they require efficient data transfer links. On the other hand, IoT devices do not require data transmission all the time. They can collect a large amount of data and transfer them together, say once a day. In this case, UAVs are considered as a competitive candidate to serve these devices [8], since they can first wirelessly charge IoT devices [9], establish LoS links, collect data efficiently based on the dynamic demand of the IoT devices and hence, prolong the lifetime of the network.

Besides communication advantages, another important application of UAVs is the on-demand transport of packages. Delivery applications include package deliveries, such as last-mile deliveries, remote areas, and door-to-door express deliveries. Drones are also expected to deliver medical products, such as drone-based contact-less COVID-19 diagnosis and testing [10], vaccines, and blood, which significantly improve the quality of medical services. Drone-based flying taxis are being tested and expected to begin commercial operations soon. Compared with a traditional truck delivery system, a drone-based system may be faster due to the lower traffic and ability to avoid low altitude obstacles and have a lower cost per mile to operate [11].

Generally, drones are typically designed to be dedicated to a single purpose. However, several demands of personal and commercial applications will cause heavy traffic conflicts in future aerial networks [5] and it is not energy- or space-efficient for all the operators to have their own physical infrastructure or own dedicated UAVs. One of the most straightforward solutions is sharing: drones can be designed more flexibly to finish multiple tasks at the same time, such as delivering a package while providing coverage [5] or transferring data. This article aims to investigate the possibilities of delivering packages and data simultaneously. With that being said, we consider an energy-limited rotary-wing UAV to finish multiple tasks simultaneously. Specifically, we use stochastic geometry and optimization tools to analyze the system performance, such as energy consumption, delivery time, total round trip time, and maximum collected/delivered data, in a general case.

Manuscript received 23 May 2022; revised 12 September 2022; accepted 28 October 2022. Date of publication 1 November 2022; date of current version 20 February 2023. This work was supported by KAUST Office of Sponsored Research. *(Corresponding author: Mustafa A. Kishk.)*

Yujie Qin and Mohamed-Slim Alouini are with the Computer, Electrical and Mathematical Sciences and Engineering Division, King Abdullah University of Science and Technology, Thuwal 23955-6900, Saudi Arabia (e-mail: yujie.qin@kaust.edu.sa; slim.alouini@kaust.edu.sa).

Mustafa A. Kishk is with the Department of Electronic Engineering, National University of Ireland, Maynooth, W23 F2H6 Ireland (e-mail: mustafa.kishk@mu.ie).

Digital Object Identifier 10.1109/JIOT.2022.3218674

A. Related Work

The literature related to this work can be categorized into: 1) UAV-enabled package delivery; 2) UAV-enabled communication networks; and 3) stochastic geometry-based analysis of UAV networks. A brief discussion on related works is provided in the following lines.

UAV-Enabled Package Delivery: Considering drone for last-mile delivery is a recent hot topic. A creation of technology road mapping for drones, used by Amazon for their latest service Amazon Prime Air, was provided in [12] and [13]. Yoo et al. [14] examined the determinants of the customer adoption of drone delivery. Agatz et al. [15] studied the traveling salesman problem. Compared to truck-only delivery, their experiment showed that substantial savings are possible by using drone-based delivery. Besides packages, drones can also be used in delivering medical supplies [16]. Ackerman and Koziol [17] mentioned that Zipline delivers blood as well as other urgent medical supplies to hospitals and clinics every day in Rwanda. Under the current situation of COVID-19, drones are beneficial in handling the pandemic since they can cover a large area and provide data, such as thermal image and patient identification [18] and contactlessly deliver the test kit to the patient having a high likelihood of infected [10]. Moreover, drone-based package delivery is expected to be cost-competitive, fast, and conveniently accessible compared to traditional ground-based delivery in or near urban regions [11], [14], [15], [19], [20], [21]. In addition to package delivery, aerial passenger transportation technology has also been progressing lately (flying taxi) [22].

UAV-Enabled Communication Networks: Otto et al. [11] comprehensively surveyed the applications of UAVs and related approaches to optimize their operations, such as path planning of area coverage, routing for a set of locations, planning of data gathering, and recharging in wireless sensor networks. Gupta et al. [9] envisaged the idea of UAVs dedicated for wireless charging of sensor networks. They presented a suitable pricing model based on a game-theoretic approach. Similarly, IoT devices are also energy-limited. Samir et al. [23] maximized the number of served IoT devices by jointly optimizing the trajectory of a UAV and radio resource allocation. Besides optimizing the trajectory of a single UAV, network architecture and the optimal number of UAVs were analyzed, and a low-latency routing algorithm was designed based on the network architecture and partial location information in [24]. Reliable uplink communications between UAVs and IoT devices with minimum transmit power were investigated in [25]. Using the proposed approach, reliability can be highly enhanced while the transmit power is sharply reduced. Xie et al. [26] investigated a throughput maximization problem in a UAV-enabled network, where UAV first wireless charges users in downlink then the user uses the harvested energy to transmit in the uplink. Mozaffari et al. [27] concluded that UAVs' altitude and the beamwidth of the antenna should be adjusted properly to mitigate interference. The possible application of UAV-enabled intelligent transportation system (ITS) was analyzed in [28], where the authors studied the applications of UAV-enabled ITS and UAV deployment and discussed the security challenges. UAVs' transmission completion time was first analyzed in [29] and the authors developed an algorithm to efficiently minimize the time. A one/two-UAV deployment strategy was analyzed in [30], where the authors computed the energy efficiency and showed that an optimal cluster pair density exists. Zhou et al. [31] studied the UAV-enabled mobile edge computing systems and showed the tradeoff between security and latency of such a system. Amer et al. [32] proposed a novel system model for cooperative transmission for UAV users. They considered UAVs as users and having frequent movements, and TBSs serving multiple UAV users.

Stochastic Geometry-Based Analysis of UAV Networks: Stochastic geometry is a strong mathematical tool that enables characterizing the statistics of various large-scale wireless networks [33], [34]. UAV-enabled fair shared spectrum access was analyzed in the coexistence of cellular users and IoT devices in [35] to maximize their energy efficiency. Alzenad and Yanikomeroglu [7], Galkin et al. [36], and Alzenad et al. [37] studied a heterogeneous network composed of TBSs and UAVs, in which the locations were modeled by two independent Poisson point processes (PPPs). Downlink coverage probability and average data rate for the considered setup were derived after accurately characterizing the Laplace transform of the interference coming from both aerial and terrestrial BSs. Another commonly used point process, "Matern cluster process (MCP)," was used in [38], [39], [40], and [41] to analyze the system performance, where users were assumed to be uniformly located within the user cluster. A stochastic geometry-based moving ABSs network was designed in [42]. The authors studied two special cases and showed that moving ABSs provide both mobility and coverage benefits. Senadhira et al. [43] proposed a novel system where aerial users periodically transmit with BSs while moving via a given trajectory and observed that the minimum height of exceeding target rates depends on the distance to the BSs. Banagar and Dhillon [44] proposed a stochastic geometry-based mobility model for UAV-enabled cellular networks, considered two mobility models, and compared their models with some more complicated model, where UAVs move in nonlinear trajectories.

While the existing literature mainly focuses on the single application of UAV-enabled network, there is a few works about integrating these functions together [5]. While Khosravi et al. [5] optimized the trajectory of UAVs when delivering packages to provide uniform coverage for the whole area, our UAVs acting as aerial wireless data relays and means of aerial transportation to deliver packages and collect/deliver data from IoT clusters simultaneously.

B. Contribution

This article systematically investigates the feasibility of integrating communication and transport functions on a single UAV and its performance. Needless to say, while we choose package and IoT devices data delivery as our main focus, this idea holds for all kinds of applications: providing coverage to user clusters, communicating with roadside units or vehicles while delivering packages or even passengers, etc. Besides, we consider all system components to be randomly located to

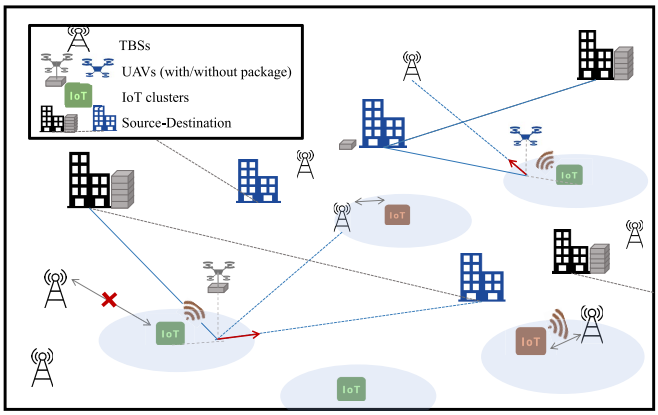

Fig. 1. Illustration of system model.

be more realistic and capture the average system performance. More detailed discussions are provided next.

Novel Framework and Performance Metrics: To solve the problem of heavy traffic conflicts in future aerial networks, we propose a novel system where UAVs are multifunctional: transferring data from IoT devices to TBSs while delivering packages. Given these two goals of this UAV network, we systematically investigate the network performance from each perspective of network components by defining delivery efficiency and computing maximum collected/delivered data and the minimum round trip time subject to UAVs' limited energy.

UAVs' Optimal Trajectory: From the perspective of operators, we optimize the trajectory of UAVs to maximize the collected/delivered IoT data and minimize the time spent in the whole trip (e.g., finish both assignments: deliver the package and transfer the data) within the limited battery energy. Unlike the existing literature, we use tools from stochastic geometry and model the locations of IoT clusters and TBSs by two independent PPPs, which is more realistic and has no restrictions on the locations. That is, our proposed algorithm for optimizing the trajectory fits different kinds of scenarios.

System-Level Insights: Since we consider all the nodes to be randomly located, our results are based on average system performance. Our results reveal that it is more time and energy efficient for UAVs to finish multitasks simultaneously. We show that the idea of integrating the aforementioned functions on single UAVs works well in general cases, which opens interesting topics in future UAV networks.

II. System Model

Given that IoT devices require reliable communication channels, which are energy limited, and usually, TBSs are too far and consume a large amount of energy, we consider a UAV delivery system that can simultaneously help IoT devices to communicate with TBSs, as shown in Fig. 1. With that being said, while UAVs deliver packages from the warehouses to residential areas (sources to the destinations), we consider them to be able to collect data from IoT devices and then forward it to the nearest TBS along the route, and the distance between the nearest TBS to the UAV trajectory is R_b (more details about the distance are provided in Section III). The locations of source and destination (S–D) pairs are modeled by Poisson bipolar networks, in which each source has a destination at a distance L_2 in a random orientation. The UAV starts at S with a package and drops off the package when it arrives at D. The locations of TBSs and IoT cluster centers are modeled by two independent PPPs Φ_t and Φ_i, with different densities λ_t and λ_i, respectively. We consider that UAVs only provide service (data collection and delivery) to the IoT clusters which are far from TBSs and their data rate (when communicating with TBSs directly without UAVs) is lower than a predefined threshold c_t.

A. Power Consumption

Consider the UAV's onboard battery limitation to be the main system's bottleneck. UAVs rely on their internal battery for power supply, hence, the amount of time they can fly/hover, providing service as well as the weight of the package they can carry is limited. Generally, the total power consumption of UAVs is composed of communication-related power and propulsion-related power. The power consumption model of this work is based on [45].

The power consumption of a rotary-wing UAV, which is sensitive to the payload and size, is given by

$$p(V) = P_0\left(1+\frac{3V^2}{U_{\text{tip}}^2}\right) + P_i\left(\sqrt{1+\frac{V^4}{4v_0^4}}-\frac{V^2}{2v_0^2}\right)^{1/2} + \frac{1}{2}d_0\rho sAV^3$$

where

$$P_0 = \frac{\delta}{8}\rho sA\Omega^3R^3$$
$$P_i = (1+k)\frac{W^{3/2}}{\sqrt{2\rho A}} \quad (1)$$

in which W is the total weight of UAVs (the sum of both aircraft and the average weight of the package $\bar{w}$), V is the velocity of UAVs, ρ is the air density, R is the rotor radius, A is the area of the rotor disc, v_0 is the mean rotor-induced velocity, U_{tip} denotes the tip speed, s is the rotor solidity, Ω is the blade angular velocity, R is the rotor radius, k is the incremental correction factor, and δ is the profile drag coefficient.

Let $p_m(V)$ and $p_s(V)$ be the motion- and service-related power of UAVs without carrying packages, and $p_{mp}(V)$ and $p_{sp}(V)$ be the motion- and service-related power of UAVs with packages. We consider that UAVs use the optimal velocities to minimize the power consumption when traveling, and let v and v_p be the optimal velocities without/with package, respectively. Besides, the service-related power of UAVs is composed of hovering and communication power, and the velocity of UAVs is 0 when hovering. Hence, in the following text, we simplify the notations and use $p_{\{m,mp,s,sp\}}$ since all the velocities are constant.

B. Communication Channel and Time Consumption

The communication channels between UAVs and 1) IoT devices (I2U) and 2) TBSs (U2B) are modeled as Nakagami-m fading channels. Given the horizontal distances between the serving UAV and IoT device, TBS are R_{i2u} and R_{u2b},

respectively, the received power of UAVs from IoT devices is given by

$$p_i(R_{\mathrm{i2u}}) = \begin{cases} p_{i,l}(R_{\mathrm{i2u}}) = \eta_l \rho_i G_l D_{\mathrm{i2u}}^{-\alpha_l}, & \text{in the case of LoS} \\ p_{\mathrm{i,n}}(R_{\mathrm{i2u}}) = \eta_n \rho_i G_n D_{\mathrm{i2u}}^{-\alpha_n}, & \text{in the case of NLoS} \end{cases} \tag{2}$$

where $D_{\mathrm{i2u}} = \sqrt{h^2 + R_{\mathrm{i2u}}}$ and h is the UAVs' altitude. Similarly, the received power of TBSs from UAVs is given by

$$p_u(R_{\mathrm{u2b}}) = \begin{cases} p_{u,l}(R_{\mathrm{u2b}}) = \eta_l \rho_u G_l D_{\mathrm{u2b}}^{-\alpha_l}, & \text{in the case of LoS} \\ p_{\mathrm{u,n}}(R_{\mathrm{u2b}}) = \eta_n \rho_u G_n D_{\mathrm{u2b}}^{-\alpha_n}, & \text{in the case of NLoS} \end{cases} \tag{3}$$

where $D_{\mathrm{u2b}} = \sqrt{h^2 + R_{\mathrm{u2b}}}$, η_l and η_n are the mean additional losses for LoS and NLoS transmissions, α_l and α_n are the path loss of LoS and NLoS links, respectively, G_l and G_n denote the fading gains that follow Gamma distribution with shape and scale parameters $(m_l, (1/m_l))$ and $(m_n, (1/m_n))$, and ρ_i and ρ_u are the transmit power of IoT devices and UAVs, respectively. The occurrence probability of LoS links and NLoS links between UAVs and serving targets (IoT devices or TBSs) are functions of Euclidean distance r, which are given in [6] as

$$\begin{aligned} P_l(r) &= \frac{1}{1 + a\exp\left(-b\left(\frac{180}{\pi}\arctan\left(\frac{h}{r}\right) - a\right)\right)}, \\ P_n(r) &= 1 - P_l(r) \end{aligned} \tag{4}$$

where a and b are two environment variables.

The fading channels between IoT devices and TBSs (I2B) are modeled as a special case of Nakagami-m fading, denoted by G_g, where the shape and scale parameters $(m_g, (1/m_g))$ are fixed as $(1, 1)$. Hence, the received power of TBSs from IoT devices directly is

$$p_b(R_{\mathrm{i2b}}) = \rho_i G_g R_{\mathrm{i2b}}^{-\alpha_t} \tag{5}$$

where α_b is the path loss and R_{i2b} is the related distance.

Consequently, for each of the IoT device and UAV, the maximum achievable rate in bps/Hz is given by

$$C(R) = \log_2\left(1 + \frac{p(R)}{\sigma^2}\right) \tag{6}$$

where $C(\cdot) \in \{C_{\mathrm{i2u}}(R_{\mathrm{i2u}}), C_{\mathrm{u2b}}(R_{\mathrm{u2b}}), C_{\mathrm{i2b}}(R_{\mathrm{i2b}})\}$ corresponding to $p(\cdot) \in \{p_i(R_{\mathrm{i2u}}), p_u(R_{\mathrm{u2b}}), p_b(R_{\mathrm{i2b}})\}$, respectively, and σ^2 is the noise power.

Let R_{c2u}, R_{u2b}, and R_{c2b} be the horizontal distances between the IoT cluster center to UAVs, UAVs to TBSs, and IoT cluster center to TBSs, respectively, and let $\bar{C}(\cdot)$ be the average maximum achievable rate (average over all the IoT devices within the cluster). $\bar{C}(\cdot)$ is given by $\bar{C}(R') = \log_2(1+\mathbb{E}_R[(p(R)/\sigma^2)])$, where $\bar{C}(\cdot) \in \{\bar{C}_{\mathrm{c2u}}(R_{\mathrm{c2u}}), \bar{C}_{\mathrm{u2b}}(R_{\mathrm{u2b}}), \bar{C}_{\mathrm{c2b}}(R_{\mathrm{c2b}})\}$.

Remark 1: We provide an explanation for the notations of R and R', $\bar{C}(\cdot)$ and $C(\cdot)$ here. R contains the distances between each of the IoT device to the serving BS, which can be UAV or TBS, R_{i2u} and R_{i2b}. R' contains the distances between the IoT cluster center to the serving BS, R_{c2u} and R_{c2b}. The reason for this notation is, each device has its own data rate and transmission time. However, when we analyze the performance, say time consumption, it is the performance of a cluster. $C(\cdot)$ is the data rate for a device while $\bar{C}(\cdot)$ is the average data rate for an IoT cluster. If the total transmission time of a whole cluster is too long, this cluster needs a UAV to help to collect/deliver data. Besides, the distance R is conditioned on R' (e.g., R_{i2u} is the function of R_{c2u}, the relations are given in Lemma 1). Hence, after we take the expectation of $C(\cdot)$ over R, we obtain $\bar{C}(\cdot)$ which is conditioned on R'.

Definition 1 (Time Consumption): For a certain IoT cluster and UAV to TBS link, by taking the expectation over the channel fading, the total transmission time is

$$T(R') = \mathbb{E}_{\mathrm{G}}\left[\frac{M_t}{\bar{C}(R')}\right] \overset{(a)}{\approx} \mathbb{E}_{\mathrm{G}}\left[\frac{M_t}{b_w \log_2(1 + \mathrm{SNR|R'})}\right] \tag{7}$$

where the subscript G denotes the channel fading, the approximation in step (a) follows from we take the expectation of R inside the logarithm operation, and $\mathrm{SNR|R'} \triangleq \mathbb{E}_R[(p(R)/\sigma^2)] = \int_r (p(r)/\sigma^2) f_{R|R'}(r)\mathrm{d}r$ (the conditional PDF is given in Lemma 1), which is a random variable because we only take the expectation over the distances and the channel fading are still random, M_t is the collected/delivered data, b_w is the bandwidth, and $T(R') \in \{T_{\mathrm{c2u}}(R_{\mathrm{c2u}}), T_{\mathrm{u2b}}(R_{\mathrm{u2b}}), T_{\mathrm{c2b}}(R_{\mathrm{c2b}})\}$ corresponds to each $\bar{C}(\cdot)$ and $p(\cdot)$ mentioned above.

As mentioned, we consider that if the average maximum achievable rate of I2B channels of an IoT cluster is lower than a predefined threshold c_t, this IoT cluster requires a UAV to deliver the data to TBSs. The density of IoT clusters requiring UAVs is λ_t', which will be computed later in this article.

C. Optimal Trajectory

The objective of this work is to optimize the UAV trajectory to maximize the collected/delivered data between IoT devices and TBSs: data collected from IoT devices and delivered to TBSs. Here, we consider that UAVs transfer all the data collected from IoT devices. That is, UAVs modify their route and hovering time to ensure that forward all the data collected from IoT devices to TBSs.

To be more realistic, we consider that the required collected/delivered data from the IoT cluster side is limited, say M. Within the limited energy of the UAV battery, we optimize the UAV trajectory to maximize the collected/delivered data while minimizing the total round trip time. In other words, for a given location of the IoT cluster and TBS, if the UAV can deliver all the data, we minimize the required time. If the UAV cannot, we maximize the collected/delivered data.

We need to clarify that UAVs do not necessarily go to IoT cluster centers and are exactly above TBSs to communicate. Instead, they can hover at nearby points to provide service, and our goal is to find the optimal hovering points (say, $\mathbf{H_1}$ to collect data from IoT clusters and $\mathbf{H_2}$ to deliver data to TBSs), which minimizes the energy consumption or the round trip time. To simplify the notation, we use $\mathbf{H_1}, \mathbf{H_2}$ to denote the locations and the same applies to $\mathbf{L_{IoT}}, \mathbf{L_{TBS}}$, the locations of IoT cluster center and TBS, which are used in the following text.

In this case, given the locations of the IoT cluster center and TBS, the objective functions are given as

$$(\mathcal{P}_1): \max_{\mathbf{H_1},\mathbf{H_2}\in\mathbb{R}^2} \frac{M_{t|\mathbf{L_{IoT}},\mathbf{L_{TBS}}}}{b_w} \quad \text{s.t. } E_t(\mathbf{H_1},\mathbf{H_2}) \le B_{\max} \tag{8}$$

where $M_{t|\mathbf{L_{IoT}},\mathbf{L_{TBS}}}$ is the conditional collected/delivered data size, $B_{\max}$ is the maximum battery size, and $E_t(\mathbf{H_1},\mathbf{H_2})$ is the total energy consumed of given trajectory.

Let T be the time for UAVs to finish the round trip (deliver the package and collect/deliver the data) and $T|\mathbf{L_{IoT}},\mathbf{L_{TBS}}$ is the conditional round trip time

$$(\mathcal{P}_2): \min_{\mathbf{H_1},\mathbf{H_2}\in\mathbb{R}^2} T|\mathbf{L_{IoT}},\mathbf{L_{TBS}} \quad \text{s.t. } E_{T|\mathbf{L_{IoT}},\mathbf{L_{TBS}}}(\mathbf{H_1},\mathbf{H_2}) \le B_{\max}, \ \frac{M_{t|\mathbf{L_{IoT}},\mathbf{L_{TBS}}}}{b_w} = \frac{M}{b_w} \tag{9}$$

where $E_{T|\mathbf{L_{IoT}},\mathbf{L_{TBS}}}(\mathbf{H_1},\mathbf{H_2})$ is the corresponding energy consumption of the trajectory, and M is the total size of the data needed to be collected from IoT devices.

To simplify the selection of parameters, we consider transferred data over bandwidth as one parameter and U2B and I2U channels use the same bandwidth. While our goal is to maximize the collected/delivered data, it refers to maximize the collected/delivered data per Hz.

Definition 2 (Optimal Hovering Points): Let $\mathbf{H_1^*},\mathbf{H_2^*}$ be the optimal hovering points for UAV to collect and deliver the data: $\mathbf{H_1^*},\mathbf{H_2^*}$ are the solutions to the objective functions $(\mathcal{P}_1)$ and $(\mathcal{P}_2)$.

Notice that the above optimization problems solve for conditional cases, conditioned on $\mathbf{L_{IoT}},\mathbf{L_{TBS}}$, but we are interested in general performance, which is defined as follows.

Definition 3 (General Case): The general system performance is given as follows:

$$\left\{T, E_{\text{total}}, \frac{M_t}{b_w}\right\} = \mathbb{E}\left[\left\{T_{\min|\mathbf{L_{IoT}},\mathbf{L_{TBS}}}, E_{\text{total}|\mathbf{L_{IoT}},\mathbf{L_{TBS}}}, \frac{M_{t|\mathbf{L_{IoT}},\mathbf{L_{TBS}}}}{b_w}\right\}\right] \tag{10}$$

where E_{total} is the energy consumption of the optimal path and the above expectation is over the locations of IoT clusters and TBSs.

As our focus in this article is on package and data delivery. Here, we define a notation ξ referring to package delivery efficiency to characterize the additional time consumed to collect and deliver data from IoT devices.

Definition 4 (Delivery Efficiency): Delivery efficiency is defined as a time fraction

$$\xi = \frac{T_{\text{data}}}{T_{\text{nodata}}} \tag{11}$$

where T_{nodata} and T_{data} are the delivery time of UAV with/without data collection.

If ξ is close to 1, it means that data collection has less impact on the package delivery, thus, high efficiency.

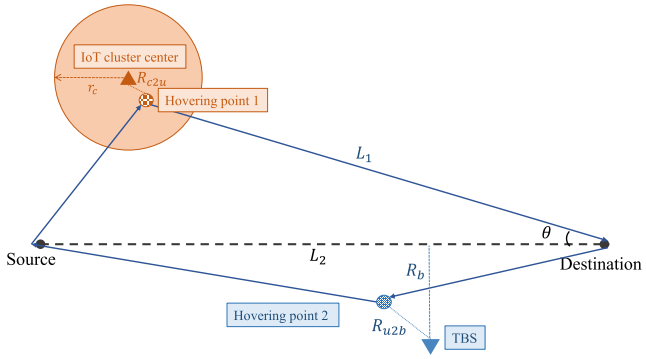

Fig. 2. Illustration of the distances.

III. Distance Distribution

Recall that R_{c2u} and R_{u2b} are the distances between the IoT cluster center to the serving UAVs and the nearest TBS, and R_b is the distance between the nearest TBS to the UAV route, as shown in Fig. 2. Before optimizing the UAV trajectory, the distance distributions are required. Remember that the communicating distance between UAVs and TBSs R_{u2b} is not a random variable since we optimize the UAV trajectory and once we obtain the $\mathbf{H_2^*}$ in Definition 2, R_{u2b} is determined and given by $R_{\text{u2b}} = ||\mathbf{L_{TBS}} - \mathbf{H_2^*}||$.

Lemma 1 (Distribution of R_{i2u} and R_{i2b}): Given the distance between the IoT cluster center and the serving UAV is R_{c2u}, in the case of $R_{\text{c2u}} > r_c$, where r_c is the radius of IoT devices cluster, the PDF of R_{i2u} is given by

$$f_{\text{R}_{\text{i2u}}}(r) = \frac{2r}{\pi r_c^2}\arccos\left(\frac{R_{\text{c2u}}^2 + r^2 - r_c^2}{2R_{\text{c2u}}r}\right) \quad \text{if} \quad R_{\text{c2u}} - r_c < r < R_{\text{c2u}} + r_c \tag{12}$$

otherwise, if $R_{\text{c2u}} \le r_c$, the PDF of R_{i2u} is

$$f_{\text{R}_{\text{i2u}}}(r) = \begin{cases} \frac{2r}{r_c^2}, & 0 < r < r_c - R_{\text{c2u}} \\ \frac{2r}{\pi r_c^2}\arccos\left(\frac{R_{\text{c2u}}^2 + r^2 - r_c^2}{2R_{\text{c2u}}r}\right), & r_c - R_{\text{c2u}} < r < R_{\text{c2u}} + r_c. \end{cases} \tag{13}$$

The PDF of R_{i2b} follows a similar distribution by conditioning on R_{c2b}, the distance between the IoT cluster center and the nearest TBS. Therefore, $f_{\text{R}_{\text{i2b}}}(r)$ can be derived directly by replacing R_{c2u} by R_{c2b}, and thus, omitted here.

As mentioned, we consider that the UAV delivers the data to the nearest TBS along the route. It means that assuming the reference UAV collecting the data from IoT devices and needs to travel to the destination to deliver the package then back to the source, the nearest TBS denotes the TBS which is the closest to UAV to **D** and **D** to **S** (**S**–**D**) segments, and R_b refers to the distance between this TBS and the nearest point on the above two segments.

Theorem 1 (Distribution of R_b): Here, we derive the CDF of R_b, which is a function of the length and the angle of the segments

$$F_{\text{R}_\text{b}}(r,\theta,L_1,L_2) = 1 - \exp\left(-\lambda_t \text{Area}(r,\theta,L_1,L_2)\right) \tag{14}$$

where

$$\begin{aligned}
&\text{Area}(r,\theta,L_1,L_2)=\text{Area}_1(r,L_2)+\text{Area}_2(r,\theta)\\
&\qquad\qquad +\text{Area}_3(r,\theta,L_1)-\text{Area}_{\text{hole}}(r)\\
&\text{Area}_1(r,L_2)=\pi r^2+2L_2r\\
&\text{Area}_2(r,\theta)=r^2\tan\left(\frac{\theta}{2}\right)-r^2\\
&\text{Area}_3(r,\theta,L_1)=\\
&\quad\begin{cases}
2r\left(L_1-\frac{r}{\sin(\theta)}\right)+\frac{r^2\pi}{2}, & 0\le r\le L_1\tan\left(\frac{\theta}{2}\right)\\
\frac{r^2(\theta_1-\sin\theta_1)}{2}+\left(L_1-r\tan\frac{\theta}{2}\right)\left(r\sin\frac{\theta_1}{2}\right)\sin\left(\frac{\theta_1}{2}\right) & \\
L_1\tan\left(\frac{\theta}{2}\right)\le r\le L_1\tan(\theta) & \\
\quad\frac{1}{2}\sin(\theta)xy+\theta_3r^2-\frac{r^2\sin(2\theta_3)}{2}, & L_1\tan(\theta)\le r
\end{cases}\\
&\text{Area}_{\text{hole}}(r)=\begin{cases}\frac{1}{2}\pi r^2+rr_t\cos(\theta_2)+\theta_2r_t^2, & r<r_t\\ \pi r_t^2, & r_t\le r\end{cases}
\end{aligned}\tag{15}$$

in which

$$\begin{aligned}
&\theta_1=\arcsin\left(\frac{l_1\sin(\theta)-r}{r}\right)+\theta+\frac{\pi}{2}\\
&\theta_2=\arcsin\left(\frac{r}{r_t}\right),\quad \theta_3=\arcsin\left(\frac{z}{2r}\right)\\
&x=l_1-r\tan\left(\frac{\theta}{2}\right),\quad y=r\sin(\theta_4)+l_1\cos(\theta)+r\tan\left(\frac{\theta}{2}\right)\\
&z=\sqrt{(y-x\cos(\theta))^2+(x\sin(\theta))^2}\\
&\theta_4=\frac{\pi}{2}-\arcsin\left(\frac{r-l_1\sin(\theta)}{r}\right)
\end{aligned}\tag{16}$$

all the related angles, lengths, and geometry relations are shown in the proof.

Proof: See the Appendix. ∎

IV. Optimal Trajectory

In this section, we mainly propose a multipurpose algorithm to solve the optimization problems $(\mathcal{P}_1)$ and $(\mathcal{P}_2)$. Recall that the objective of this work is data collection while delivering the package, we first maximize the size of collected data. If it is beyond the requirement of IoT devices, we minimize the round trip time while delivering all the data. To do so, we first need to characterize the time consumption when transferring the data.

Observing that the time consumption defined in Definition 1 requires to take the expectation over SNR. Using the following lemma, we derive the PDF of SNR.

Lemma 2 (PDF of SNR): Coverage probability is the CCDF of SNR, given by

$$\begin{aligned}
P_{\text{cov}|\text{R}'}=\mathbb{P}\left(\frac{p(R)}{\sigma^2}>\gamma\right)=\int_r\Bigg(&\sum_{k=0}^{m_l}\frac{\left(m_lg_l\left(\sqrt{r^2+h^2}\right)\gamma\right)^k}{k!}\\
&P_l\left(\sqrt{r^2+h^2}\right)\exp\left(-m_lg_l\left(\sqrt{r^2+h^2}\right)\gamma\right)\\
&+\sum_{k=0}^{m_n}\frac{\left(m_ng_n\left(\sqrt{r^2+h^2}\right)\gamma\right)^k}{k!}\\
&P_n\left(\sqrt{r^2+h^2}\right)\exp\left(-m_ng_n\left(\sqrt{r^2+h^2}\right)\gamma\right)\Bigg)f_R(r)\text{d}r
\end{aligned}$$

$$\begin{aligned}
P_{\text{cov}|\text{R}_{\text{u2b}}}=\mathbb{P}\left(\frac{p_u(R_{\text{u2b}})}{\sigma^2}>\gamma\right)=\Bigg(&\sum_{k=0}^{m_l}\frac{\left(m_lg_l\left(\sqrt{R_{\text{u2b}}^2+h^2}\right)\gamma\right)^k}{k!}\\
&P_l\left(\sqrt{R_{\text{u2b}}^2+h^2}\right)\exp\left(-m_lg_l\left(\sqrt{R_{\text{u2b}}^2+h^2}\right)\gamma\right)\\
&+\sum_{k=0}^{m_n}\frac{\left(m_ng_n\left(\sqrt{R_{\text{u2b}}^2+h^2}\right)\gamma\right)^k}{k!}P_n\left(\sqrt{R_{\text{u2b}}^2+h^2}\right)\\
&\times\exp\left(-m_ng_n\left(\sqrt{R_{\text{u2b}}^2+h^2}\right)\gamma\right)\Bigg)
\end{aligned}\tag{17}$$

where $g_l(r)=\gamma(\rho\eta_l)^{-1}r^{\alpha_l}$ and $g_n(r)=\gamma(\rho\eta_n)^{-1}r^{\alpha_n}$, $\rho\in\{\rho_i,\rho_u\}$ depends on IoT or UAV communication and corresponding to $p\in\{p_i(R_{\text{i2u}}),p_b(R_{\text{i2b}})\}$, $R'\in\{R_{\text{c2u}},R_{\text{c2t}}\}$, and $R\in\{R_{\text{i2u}},R_{\text{i2b}}\}$. Hence, the PDF of SNR is derived by taking the first derivative of CCDF

$$\begin{aligned}
f_{\text{SNR}|\text{R}'}(\gamma)=&\sum_{k=1}^{m_l-1}\int_r\frac{\left(m_lg_l\left(\sqrt{r^2+h^2}\right)\right)^k}{k!}P_l\left(\sqrt{r^2+h^2}\right)\\
&\exp\left(-m_lg_l\left(\sqrt{r^2+h^2}\right)\gamma\right)f_R(r)\left(m_lg_l\left(\sqrt{r^2+h^2}\right)\gamma^k-k\gamma^{k-1}\right)\text{d}r\\
&+\sum_{k=1}^{m_n-1}\int_r\frac{\left(m_ng_n\left(\sqrt{r^2+h^2}\right)\right)^k}{k!}P_n\left(\sqrt{r^2+h^2}\right)\\
&\exp\left(-m_ng_n\left(\sqrt{r^2+h^2}\right)\gamma\right)f_R(r)\left(m_ng_n\left(\sqrt{r^2+h^2}\right)\gamma^k-k\gamma^{k-1}\right)\text{d}r,\\
f_{\text{SNR}|\text{R}_{\text{u2b}}}(\gamma)=&\sum_{k=1}^{m_l-1}\frac{\left(m_lg_l\left(\sqrt{R_{\text{u2b}}^2+h^2}\right)\right)^k}{k!}P_l\left(\sqrt{R_{\text{u2b}}^2+h^2}\right)\\
&\times\exp\left(-m_lg_l\left(\sqrt{r^2+h^2}\right)\gamma\right)\left(m_lg_l\left(\sqrt{R_{\text{u2b}}^2+h^2}\right)\gamma^k-k\gamma^{k-1}\right)\\
&+\sum_{k=1}^{m_n-1}\frac{\left(m_ng_n\left(\sqrt{R_{\text{u2b}}^2+h^2}\right)\right)^k}{k!}P_n\left(\sqrt{R_{\text{u2b}}^2+h^2}\right)\\
&\exp\left(-m_ng_n\left(\sqrt{R_{\text{u2b}}^2+h^2}\right)\gamma\right)\left(m_ng_n\left(\sqrt{R_{\text{u2b}}^2+h^2}\right)\gamma^k-k\gamma^{k-1}\right).
\end{aligned}\tag{18}$$

Note that the PDF of SNR of the U2B channel is different from I2U and I2B channels owing to that R_{u2b} is not a random variable.

Proof: The coverage probability equation is derived by the fact that 1) $\bar{F}_{\text{G}}(g)=(\Gamma_u(m,g)/\Gamma(m))$, where $\Gamma_u(m,g)=\int_{mg}^{\infty}t^{m-1}e^{-t}dt$ is the upper incomplete Gamma function and 2) $(\Gamma_u(m,g)/\Gamma(m))=\exp(-g)\sum_{k=0}^{m-1}(g^k/k!)$. ∎

Using the PDF of SNR derived above, we can now obtain the density of IoT clusters that need UAVs numerically

$$\lambda_i'=\lambda_i\exp\left(-\pi\lambda_tr_t^2\right)\tag{19}$$

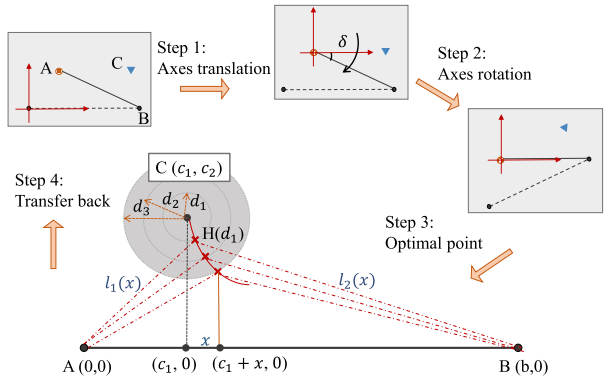

Fig. 3. Illustration of finding the optimal hovering point.

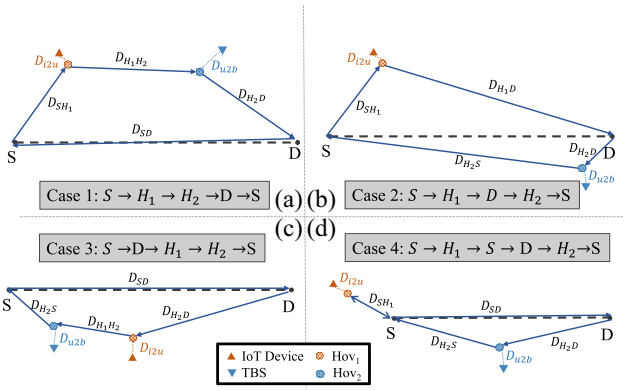

Fig. 4. Illustration of four possible trajectories of UAVs. Note that 1) H_1 and H_2 refer to hovering points $H_1(R_{\mathrm{c2u}})$ and $H_2(R_{\mathrm{u2b}})$ and 2) $\mathbf{Hov}_1(R_{\mathrm{c2u}})$ and $\mathbf{Hov}_2(R_{\mathrm{u2b}})$ are the optimal hovering points for each case, but not the final solutions to $(\mathcal{P}_1)$ and $(\mathcal{P}_2)$.

where r_t is the solution of x to the following function:

$$\int_0^{\infty} \bar{C}_{\mathrm{c2b}}(x) f_{\mathrm{SNR}|\mathrm{R}'}(\gamma)\mathrm{d}\gamma = c_t. \tag{20}$$

Recall that $M_{t|\mathbf{L_{IoT}},\mathbf{L_{TBS}}}$ is the actual data UAV collected and delivered, which is smaller or equal to M. We now compute the time consumption of each link.

Theorem 2 (Time Consumption): Following Definition 1, we take the expectation over SNR using the PDF derived above, the time consumption given the distance is

$$T(R') = \frac{M_{t|\mathbf{L_{IoT}},\mathbf{L_{TBS}}}}{b_w} \int_0^{\infty} \frac{1}{\log_2(1+\mathrm{SNR}|\mathrm{R}')} f_{\mathrm{SNR}|\mathrm{R}'}(\gamma)\mathrm{d}\gamma \tag{21}$$

where $T(\cdot) \in \{T_{\mathrm{c2u}}(R_{\mathrm{c2u}}), T_{\mathrm{u2b}}(R_{\mathrm{u2b}}), T_{\mathrm{c2b}}(R_{\mathrm{c2t}})\}$.

We then minimize the UAV path which results in minimum traveling time and energy consumed during traveling. Suppose now the reference UAV travels from **A** to **B** while hovering at $\mathbf{H}(d)$ to communicate with **C** at d away, and we aim to find the optimal $\mathbf{H}^*(d)$ that minimizes the length of the path

$$\mathbf{H}^*(d) = \arg\min_{|(\mathbf{H}(d)-\mathbf{C})|=d} |\mathbf{A}-\mathbf{H}(d)| + |\mathbf{H}(d)-\mathbf{B}|. \tag{22}$$

In what follows, we find the shortest path of UAV given R_{c2u} and R_{u2b}.

Lemma 3 (Shortest Path): Let $\mathbf{Hov}_1(R_{\mathrm{c2u}})$ and $\mathbf{Hov}_2(R_{\mathrm{u2b}})$ be the hovering points which minimize the trajectory of UAV given the distances R_{c2u} and R_{u2b}, respectively. The steps of obtaining $\mathbf{Hov}_1(R_{\mathrm{c2u}})$ and $\mathbf{Hov}_2(R_{\mathrm{u2b}})$ are shown in Fig. 3.

Proof: Our goal here is to find the optimal point $\mathbf{Hov}_{\{\mathbf{1},\mathbf{2}\}}(d)$ which minimizes the length of the target trajectory given the final distance between **C** and UAV is d. We first establish a new coordinate system whose origin is A and the x-axis is $\vec{AB}$, as step 1 and step 2, the relationship of these two coordinates is the superposition of a rotation matrix and a translation vector

$$\begin{bmatrix} x' \\ y' \end{bmatrix} = \begin{bmatrix} \cos\delta & \sin\delta \\ -\sin\delta & \cos\delta \end{bmatrix} \begin{bmatrix} x \\ y \end{bmatrix} - A \tag{23}$$

where x' and y' are new coordinates and x, y are the original coordinates, and δ is the counter clockwise.

Based on the geometry relation shown in Fig. 3, the shortest length can be derived numerically in step 3

$$\begin{aligned} l^* &= \min l(x) = l_1(x) + l_2(x) \\ &= \min \sqrt{(c_1+x)^2 + \left(c_2 - \sqrt{d-x^2}\right)^2} \\ &\quad + \sqrt{(b-c_1-x)^2 + \left(c_2 - \sqrt{d-x^2}\right)^2} \end{aligned} \tag{24}$$

the above equation solved by setting $(\mathrm{d}l(x)/\mathrm{d}x) = 0$ and $x^* = \arg\min l(x)$.

Finally, transfer the coordination system back to the original one and we obtain $\mathbf{Hov}_1(R_{\mathrm{c2u}})$ and $\mathbf{Hov}_2(R_{\mathrm{u2b}})$ given serving distance. ■

Now that we are ready for our algorithm and final solutions to the optimization problems. We divide the UAV trajectory into four possible routes, as shown in Fig. 4, and each of the total energy consumption and time needed are given below, where $D_{\{\cdot\}}$ are distances, and the subscript H_1 and H_2 refer to hovering points $\mathbf{Hov}_1(R_{\mathrm{c2u}})$ and $\mathbf{Hov}_2(R_{\mathrm{u2b}})$.

Route 1: $S \to IoT \to TBS \to D \to S$: (The reference UAV starts at **S**, collects and delivers the data, and then delivers the package and finally back to **S**)

$$\begin{aligned} T_1 &= \frac{D_{\mathrm{SH}_1} + D_{H_1H_2} + D_{H_2D}}{v_p} \\ &\quad + T_{\mathrm{c2u}}(R_{\mathrm{c2u}}) + T_{\mathrm{u2b}}(R_{\mathrm{u2b}}) + \frac{D_{\mathrm{SD}}}{v}, \\ E_{t1} &= \frac{D_{\mathrm{SH}_1} + D_{\mathrm{H}_1\mathrm{H}_2} + D_{H_2D}}{v_p} p_{mp} \\ &\quad + (T_{\mathrm{c2u}}(R_{\mathrm{c2u}}) + T_{\mathrm{u2b}}(R_{\mathrm{u2b}}))p_{sp} + \frac{D_{\mathrm{SD}}}{v} p_m. \end{aligned} \tag{25}$$

Route 2: $S \to IoT \to D \to TBS \to S$: (The reference UAV starts at **S**, collects the data, and delivers the package, then delivers the data, and finally back to **S**)

$$\begin{aligned} T_2 &= \frac{D_{\mathrm{SH}_1} + D_{\mathrm{H}_1\mathrm{D}}}{v_p} + T_{\mathrm{c2u}}(R_{\mathrm{c2u}}) + T_{\mathrm{u2b}}(R_{\mathrm{u2b}}) \\ &\quad + \frac{D_{H_2D} + D_{H_2S}}{v}, \\ E_{t2} &= \frac{D_{\mathrm{SH}_1} + D_{\mathrm{H}_1\mathrm{D}}}{v_p} p_{mp} + T_{\mathrm{c2u}}(R_{\mathrm{c2u}})p_{sp} + T_{\mathrm{u2b}}(R_{\mathrm{u2b}})p_s \\ &\quad + \frac{D_{H_2D} + D_{H_2S}}{v} p_m. \end{aligned} \tag{26}$$

Route 3: $S \to D \to IoT \to TBS \to S$ (The reference UAV starts at **S**, delivers the package first, then collects and delivers the data and finally back to **S**)

$$T_3 = \frac{D_{\mathrm{SH}_2} + D_{\mathrm{H}_1\mathrm{H}_2} + D_{\mathrm{DH}_1}}{v} + T_{\mathrm{c2u}}(R_{\mathrm{c2u}}) + T_{\mathrm{u2b}}(R_{\mathrm{u2b}}) + \frac{D_{\mathrm{SD}}}{v_p},$$

$$E_{t3} = \frac{D_{\mathrm{SH}_2} + D_{\mathrm{H}_1\mathrm{H}_2} + D_{\mathrm{DH}_1}}{v} p_m + (T_{\mathrm{c2u}}(R_{\mathrm{c2u}}) + T_{\mathrm{u2b}}(R_{\mathrm{u2b}}))p_s + \frac{D_{\mathrm{SD}}}{v_p} p_{mp}. \quad (27)$$

Route 4: $S \to IoT \to S \to D \to TBS \to S$ (The reference UAV starts at **S**, collects the data first, then back to **S** to take the package and delivers the data and package)

$$T_4 = \frac{2D_{\mathrm{SH}_1} + D_{\mathrm{SH}_2} + D_{H_2D}}{v} + T_{\mathrm{c2u}}(R_{\mathrm{c2u}}) + T_{\mathrm{u2b}}(R_{\mathrm{u2b}}) + \frac{D_{\mathrm{SD}}}{v_p},$$

$$E_{t4} = \frac{2D_{\mathrm{SH}_1} + D_{\mathrm{SH}_2} + D_{H_2D}}{v} p_m + (T_{\mathrm{c2u}}(R_{\mathrm{c2u}}) + T_{\mathrm{u2b}}(R_{\mathrm{u2b}}))p_s + \frac{D_{\mathrm{SD}}}{v_p} p_{mp}. \quad (28)$$

In the following text, we propose an algorithm that solves the optimization problems given $\mathbf{L_{IoT}}$ and $\mathbf{L_{TBS}}$, as shown in Algorithm 1. The detailed steps are provided in the following text.

We first find the distance between $\mathbf{L_{IoT}}$ to nearest point on **S–D** segment is $R_{\max}$. Our algorithm starts from conditioning on each $R_{\mathrm{c2u}} \in (0, R_{\max})$. For each R_{c2u}, we obtain $\mathbf{Hov_1}$ using Lemma 3.

Variables and Notations: E_{con}, T_{Mmax}, T_{total}, and $M_{\max}$ are the temporary variables used in iterations. Let Φ_{Hov_1} be the point set of $\mathbf{Hov_1}$, and let $\Phi_{\mathrm{Hov}_2|\mathrm{Hov}_1}$ be the point set of $\mathbf{Hov_2}$ given $\mathbf{Hov_1}$. In addition, this algorithm solves the conditional optimization problem: all the outputs are actually conditioned to the locations of the IoT cluster and TBS. However, to simplify the notation, here we use M_t instead of $M_{\mathrm{t}|\mathbf{L_{IoT}},\mathbf{L_{TBS}}}$ and the same applies to E_{total} and T. As mentioned, we consider the transmitted data over bandwidth as one parameter, therefore, $M_{\{\cdot\}}$ refers to $(M_{\{\cdot\}}/b_w)$.

Part 1 (Maximum Transferred Data): We first check the maximum data $M_{\max}$ that UAV can transfer for given R_{c2u}. Notice that the time consumption of collecting data T_{c2u} and T_{u2b} is only the functions of the distances R_{c2u} and R_{u2b} (assume that (M/b_w) and ρ_i are predetermined) and $\mathbf{Hov_1}$ can be obtained by using Lemma 3. Therefore, the optimal R_{u2b} and corresponding $\mathbf{Hov_2}$ that maximize $M_{\max}$ given R_{u2b} can be easily obtained. R_{u2b} is derived by solving

$$\frac{M_{\max}}{b_w} = \frac{\left(B_{\max} - \frac{l_p}{v_p} p_{mp} - \frac{l}{v} p_m\right)}{T_{\mathrm{c2u}}(R_{\mathrm{c2u}})p_{\{s,sp\}} + T_{\mathrm{u2b}}(R_{\mathrm{u2b}})p_{\{s,sp\}}} \quad (29)$$

where l and l_p are the traveling distances with/without package, and the denominator p_{sp} or p_s is owing to the states of UAVs when communicating: with or without package, and $\mathbf{Hov_2}$ is obtained by Lemma 3.

Algorithm 1: Algorithm for UAV Optimal Route Planning

Input: M: Required transmitted data
($\mathrm{IoT_x}$, $\mathrm{IoT_y}$): Location of IoT cluster center
($\mathrm{TBS_x}$, $\mathrm{TBS_y}$): Location of TBS
Output: T: Minimum time to finish the assisgnment
H_1^*, H_2^*: Locations of UAV hovering to provide service
$\mathrm{M_t}$: Maximum collected/delivered data
$\mathrm{E_{total}}$: Energy consumption of UAV
Route: Route of UAVs
Initialization: $\mathrm{T} = \infty$, $E_{\mathrm{total}} = \infty$, $\mathrm{M_t} = 0$, $\mathrm{H}_1^* = \emptyset$, $\mathrm{H}_2^* = \emptyset$, Route $= 0$
Function `OptimalRoute`$(M, (\mathrm{IoT_x}, \mathrm{IoT_y}), (\mathrm{TBS_x}, \mathrm{TBS_y}))$**:**
  Step 1: Find the distance $R_{\max}$ from $(\mathrm{IoT_x}, \mathrm{IoT_y})$ to the closest point on S-D segment.
  R_{u2b} given k-th iteration is $k \times step$, where $step$ is the iteration step and $k_{\max} = \frac{R_{\max}}{step}$.
  foreach $k \le k_{\max}$ **do**
    Within the limited energy, find $\mathbf{Hov_2}^{(1)}$ among 4 possible UAV routes which maximizes the transmitted data $\mathrm{M_{max}}$.
    Go to the next loop if $\mathrm{M_{max}} < 0$.
    if $M_{\max} \le M$ **then**
      Update outputs if $\mathrm{M_{max}}$ is larger than previous iterations.
    else
      Find $\mathbf{Hov_2}^{(2)}$ which minimizes the total $\mathrm{T_{total}}$ while transmitting all the data within the limited energy.
      If $M_t < M$, outputs update and $M_t = M$.
      If $M_t = M$, outputs update if T_{total} is shorter than previous iterations.
    end
  end
  return T, H_1^*, H_2^*, $\mathrm{M_t}$, $\mathrm{E_{total}}$, Route
End Function

Part 2 (Outputs Update): We then compare $M_{\max}$ with M. If $M_{\max} < M$, which means that the UAV is unable to collect and transmit all the data. In this case, we update M_t as well as all the outputs, only if $M_{\max}$ is greater than M_t. (M_t saves the largest value of $M_{\max}$ in the previous loops if none of them are greater than M; otherwise, it equals to M.) If $M_{\max} > M$, which means that the UAV is able to transfer all the data from IoT devices to the TBS within the available time and energy. In this case, we first obtain the subset $\Phi'_{\mathrm{Hov}_2|\mathrm{Hov}_1}$ of $\Phi_{\mathrm{Hov}_2|\mathrm{Hov}_1}$ which is the set of $\mathbf{Hov_2}$ that can transfer all M. Within $\Phi'_{\mathrm{Hov}_2|\mathrm{Hov}_1}$, we then find the optimal $\mathbf{Hov_2}^{(2)}$ which minimizes the round trip time T_{total} and outputs update if T_{total} is less than the previous value.

Before we process the next step is to obtain the average round trip time, energy consumption, and maximum transmitted data. We would like to clarify the goal of the above algorithm is to obtain the optimal trajectory: for a given location of the IoT cluster and TBS, if the UAV can deliver all

the data, we minimize the required time; if the UAV cannot, we maximize the collected/delivered data. This optimal trajectory can be either Route 1, 2, 3, or 4, which depends on the locations.

The above algorithm conditions on $\mathbf{L_{IoT}}$ and $\mathbf{L_{TBS}}$ which are random variables in our system, and we are interested in the power consumption, minimum round trip time, and collected/delivered data in a general case and the average system performance. However, it is difficult to obtain the joint PDF of the locations of the IoT cluster and the nearest TBS, especially when they are correlated; hence, the method in Definition 3 is hard to compute. Alternatively, we use the method provided below, which is an upper bound of the system's performance.

Theorem 3 (General Case): We first take the integral over $\mathbf{L_{TBS}}$. Since the UAV goes to the nearest TBS along the route, hence, we should take the integral over R_b, which is

$$\left\{T|\mathbf{L_{IoT}}, E_{\text{total}|\mathbf{L_{IoT}}}, \frac{M_{\text{t}|\mathbf{L_{IoT}}}}{b_w}\right\} = \int_0^\infty \left\{T_{\min|\mathbf{IoT},\mathbf{TBS}}, E_{\text{total}|\mathbf{L_{IoT}},\mathbf{L_{TBS}}}, \frac{M_{\text{t}|\mathbf{L_{IoT}},\mathbf{L_{TBS}}}}{b_w}\right\} \times F_{\text{Rb}}(r, \theta, l_1, L_2)\text{d}r \tag{30}$$

where $l_1 = ||\mathbf{L_{IoT}} - \mathbf{D}||$ and $\theta = \arccos([(L_2 - \mathbf{L_{IoT}}_x)/(||\mathbf{L_{IoT}} - \mathbf{D}||)])$.

We then use the same method and take the integral over the location of $\mathbf{L_{IoT}}$. While we admit that UAVs can provide the service to any IoT clusters which are far from TBSs, here we only consider the nearest one, the nearest to **S**–**D** pair

$$\left\{T, E_{\text{total}}, \frac{M_t}{b_w}\right\} = \int_0^\infty \left\{T|\mathbf{L_{IoT}}, E_{\text{total}|\mathbf{L_{IoT}}}, \frac{M_{\text{t}|\mathbf{L_{IoT}}}}{b_w}\right\} F_{\text{IoT}}(r)\text{d}r \tag{31}$$

where

$$F_{\text{IoT}}(r) = F_{\text{Rb}}(r, 0, 0, L_2) \tag{32}$$

and replace λ_t by λ_i'.

Remark 2: Observing that the conditional system parameters in (30) and (31) are the outputs of $(\mathcal{P}_1)$ and $(\mathcal{P}_2)$ and functions of the integral variable r which cannot be obtained in the closed form. Therefore, to solve the integration in Theorem 3, the Monte Carlo integration method is used and we provide an algorithm to solve the above integration, as shown in Algorithm 2. In addition, we only know the probability of the distance to the nearest TBS and IoT cluster center instead of the exact location (e.g., the probability of R_b instead of $\mathbf{L_{TBS}}$). Hence, in our codes, we use the upper bound: the longest route (e.g., taking route 1, for example, UAV travels from IoT cluster to TBS then to destination, and the distance between $\mathbf{L_{IoT}}$-**D** segment and TBS is R_b. The shortest path for UAV is when TBS is located at the perpendicular bisector, and the longest path is when TBS is located at the opposite point on the extension of $\mathbf{L_{IoT}}$-**D** segment), as shown in Fig. 5.

V. Numerical Results

In this section, we validate our analytical results with simulations and evaluate the impact of various system parameters

Algorithm 2: Algorithm for Monte Carlo Integration

Input: r: Integral variable
Output: T(r): Round trip time
M(r): Collected/delivered data
E(r): Energy consumption
Function `MonteCarloIntegration(r)`**:**
  Generate a vector for the values of R_b:
  $X_{\text{R}_{\text{b,1}}}, \ldots, X_{\text{R}_{\text{b,n}}}$
  Corresponding CDF ($\mathbb{P}(R_b < X_{\text{R}_{\text{b,i}}})$):
  $F_{X_{\text{R}_{\text{b,1}}}}, \ldots, F_{X_{\text{R}_{\text{b,n}}}}$
  foreach $k \leq$ iteration **do**
    Generate $U \sim$ Uniform(0, 1)
    Find the nearest point in $F_{X_{\text{R}_{\text{b,i}}}}$
    Find corresponding $X_{\text{R}_{\text{b,i}}}$
    Using Algorithm 1, find the optimal Tmin, E_{total} and M_t
  end
  Find the mean: $T(r) = \text{mean}(Tmin)$, $E(r) = \text{mean}(E_{\text{total}})$, $M(r) = \text{mean}(M_t)$ **return** $T(r), M(r), E(r)$
End Function

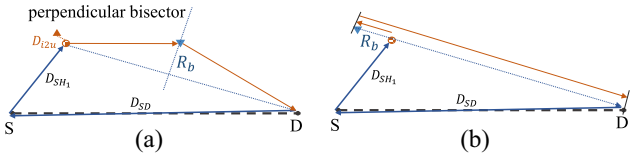

Fig. 5. Proof for the upper bound. (a) Shortest path: when TBS is located at the perpendicular bisector and (b) longest path: when TBS is located at the opposite point on the extension of $\mathbf{L_{IoT}}$-**D** segment.

TABLE I
Table of Parameters

Parameter	Symbol	Simulation Value
Density of TBS and IoT cluster	λ_{t},λ_{i}	1 km^{-2}
IoT cluster radius	r_c	50 m
Achievable rate threshold	c_t	1 bps/Hz
Average package weitht	$\bar{w}$	1 kg
Optimal with/without package velocity	v_p, v	12.4, 10 m/s
Serving-related power (with/without package)	p_s, p_{sp}	252 J, 178 J
Traveling-related power (with/without package)	p_m, p_{mp}	193 J, 159 J
UAV altitude	h	100 m
Battery capacity	$B_{\max}$	177.6 W·H
N/LoS environment variable	a, b	4.9 0.43
Transmission power	$\rho_{\text{i}}, \rho_{\text{u}}$	0.1 mW, 0.1 W
Noise power	σ^2	10^{-9} W
N/LoS and TBS path-loss exponent	$\alpha_{\text{n}}, \alpha_{\text{l}}, \alpha_{\text{t}}$	4, 2.1, 4
N/LoS fading gain	$m_{\text{n}}, m_{\text{l}}$	1, 3
N/LoS additional loss	$\eta_{\text{n}}, \eta_{\text{l}}$	$-20, 0$ dB

on the network performance. Unless stated otherwise, we use the simulation parameters as listed herein Table I.

In our simulation, we first generate the locations of IoT cluster centers, TBSs, and the locations of IoT devices. For each realization, we use Algorithm 1 to obtain the optimal route, as mentioned it can be either Route 1, 2, 3, or 4, which depends on the locations. We also obtain the maximum transferred data, round trip time, package delivery time, and the energy consumption of the optimal trajectory. Finally, we run a large number of iterations to ensure accuracy and obtain the average performance.

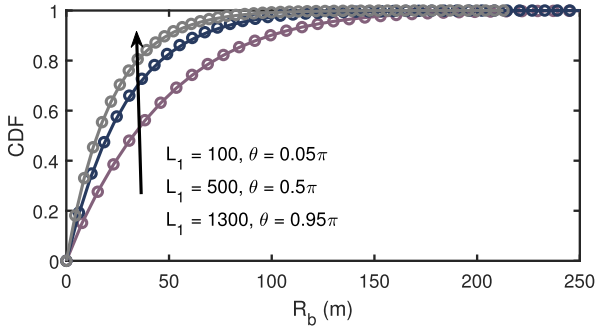

Fig. 6. Simulation results versus analysis results of the distribution of R_b, conditioned on $L_2 = 1000$ m.

For the simulation of the considered system setup, we first compute the accuracy of the distribution of R_b, as derived in Theorem 1. For given $L_2 = 1$ km, we plot the CDF of R_b under three different L_1 and θ, as shown in Fig. 6. We then use this distribution in the final Monte Carlo integration of R_b and $\mathbf{L_{IoT}}$.

In Fig. 7, we plot the average total energy consumption, average maximum collected/delivered data, and the average minimum round trip time. We first clarify that the gaps between simulation and analysis results are due to the fact that we use the upper bound in Monte Carlo integration, as mentioned in Remark 2. Besides, we only plot one analysis curve ($L_2 = 7$ km, dashed line). This is because the analysis results are the upper bound of the simulation results and the same trend applies to all distances. All the analysis results are slightly higher than the simulation results.

The maximum collected/delivered data and minimum round trip time, as expected, increase with the increase of required data until the maximum achievable value, which is limited by the onboard battery of UAVs. Total energy consumption, however, shows a different trend. This is because our goal in this work is to maximize the delivered data and minimize the round trip time within the limited energy of UAVs instead of minimizing the energy consumption of UAVs. Moreover, the minimum time path is different from the minimum energy consumption path and the maximum collected/delivered data path. This is because of the different optimal velocities and power consumption of UAVs with/without the package. Observing that UAVs with the package have higher velocity but higher energy consumption. In this case, the required transmitted data size is low and the UAV prefers to choose the trajectory that has minimal distance even if it results in higher energy consumption. However, if the transmitted data size is large, the UAV has to deliver the package first to save energy to deliver data.

To further illustrate the trend of total energy consumption, we take route 1 and route 4, for example. From the perspective of time, route 1 seems better since UAVs collect and deliver the data on the way of delivering the package. However, on the side of energy consumption, route 4 may result in less traveling, and hovering energy since the energy consumption of UAVs is very sensitive to the total weight. Therefore, traveling without a package can save a large amount of energy. In the case when IoT devices require to transfer a large amount of data, UAVs prefer route 4 owing to having more energy left to collect and deliver the data.

Fig. 8 shows the distribution of package delivery time, and delivery efficiency under different **S–D** distances and required transmitted data sizes. Interestingly, $L_2 = 3$ km achieves the lowest delivery efficiency with the shortest delivery time. The results can be explained as 1) delivery time T_{nodata} in the case of L_2 is the shortest, hence, the denominator of ξ (3 km) is the lowest and 2) when L_2 is short, the nearest IoT cluster is likely to be located further away, the same as the nearest TBS, which means that UAVs need to fly for a larger circle to transfer data.

Observing that the delivery efficiency first decreases with the increased required collected/delivered data and then decreases. The same reason as the trend of energy consumption: when the requirement collected/delivered data size is large, UAVs prefer to deliver the package first in this case they can have more energy left to collect and transfer the data. That is, with the increase of the required transferred data, UAVs spend a longer time on data transmission; with further increase of the required transferred data, UAVs deliver the package first to save energy to transfer more data.

Another attractive phenomenon in Fig. 8 is the delivery time gap. This is because the transmission time is relatively much longer than the delivery time. The low value of delivery time (left-hand side bars) is caused by the UAV delivering the package first, hence, the delivery time is only composed of the traveling time; and the high value of delivery time (right-hand side bars) is caused by the UAV transferring data (collecting data from IoT devices), hence, the delivery time is composed of communication time and traveling time.

Before concluding this section, we also discuss why not just deliver the package first and then deliver the data. To answer this question, we provide the following comparison between the energy consumption, round trip time, and maximum transferred data, from the perspective of operators, in Table II. These four points are obtained given the required transmission data are M/bw $= [1, 4, 6, 10] \times 10^3$ bit/Hz and $L_2 = 5$ km. When the required collected/delivered data size is small, delivering the package first can save UAVs' energy while the round trip time is slightly longer. However, when the required collected/delivered data is large, the maximum possible delivered data of delivering the package first is lower and the total round trip time is longer, compared to the optimal trajectory. The results in Table II reveal a tradeoff between higher quality of delivery package and higher time and energy efficiency. If the operators hope to deliver more packages, then the optimal trajectory is better, however, the relative package delivery time is longer.

VI. Conclusion

This article presented a novel system model in which UAVs simultaneously perform multiple tasks: data collection/delivery and package delivery. We investigated the possibility for UAVs to deliver the data and packages at the same time and provided an algorithm to maximize the possible collected/delivered data while minimizing the round trip time. Moreover, our system

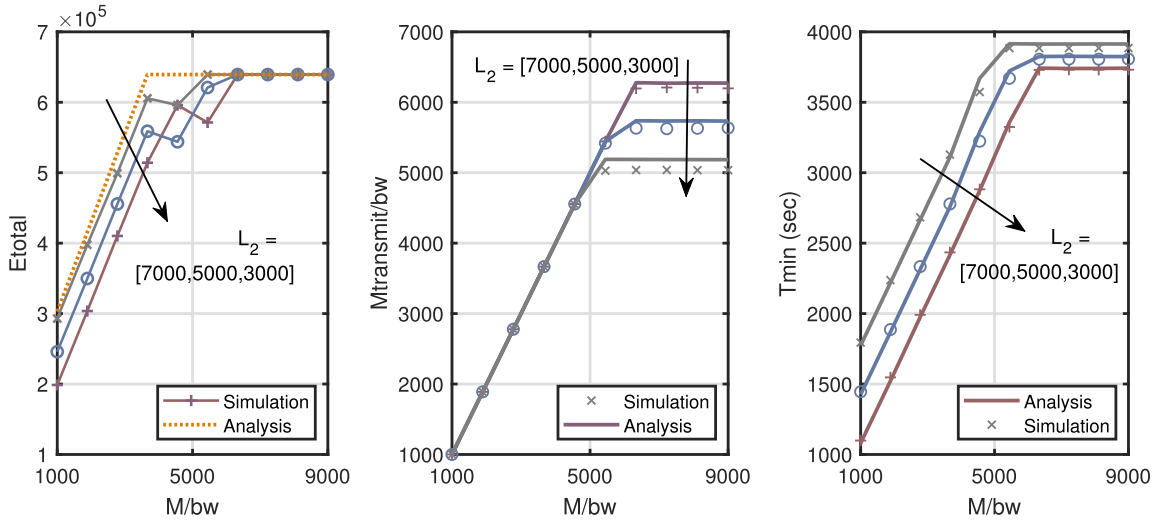

Fig. 7. Simulation and analysis results of total energy consumption, maximum collected/delivered data, and minimum round trip time versus required data from IoT devices side under different **S-D** distances. Note that we only plot one analysis result ($L_2 = 7000$ km) in energy consumption figure.

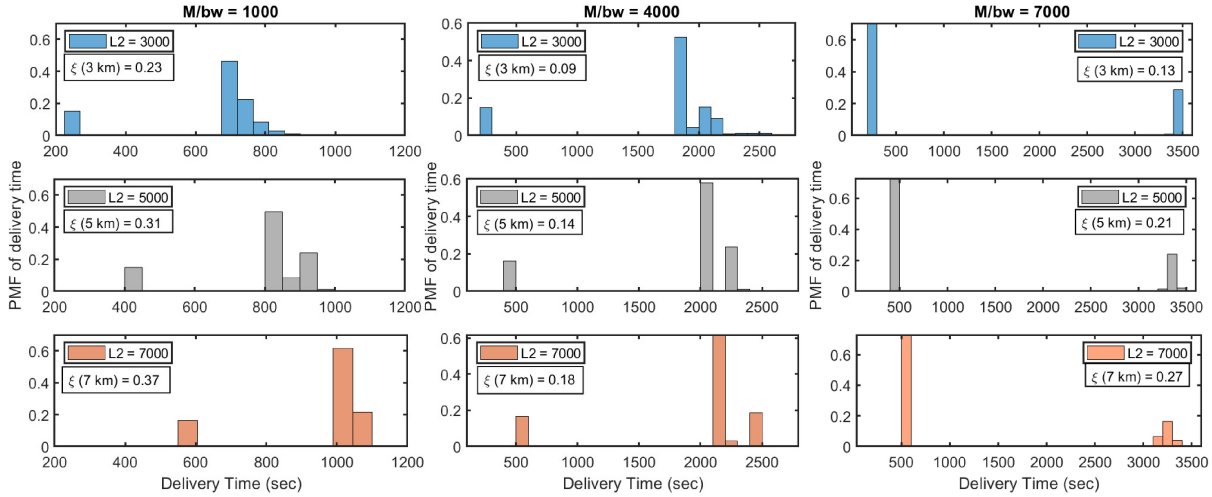

Fig. 8. Probability of delivery time and delivery efficiency under different L_2 and required amount of data.

TABLE II
COMPARISON ($L_2 = 5$ KM)

Method	**Energy Consumption** (10^5) J
Deliver package first	(2.39, 4.76, 6.4, 6.4)
Optimal trajectory	(2.45, 5.59, 6.4, 6.4)
Method	**Max Data Transferred** (10^3) bits/Hz
Deliver package first	(1, 3.7, 5.4, 5.4)
Optimal trajectory	(1, 3.7, 5.6, 5.6)
Method	**Total Time** (10^3) sec
Deliver package first	(1.6, 2.9, 3.9, 3.9)
Optimal trajectory	(1.4, 2.7, 3.8, 3.8)

model and results are applied to different scenarios since all the locations are random.

This work tapped a new aspect of the applications of UAVs. Instead of dedicated UAVs, multipurpose drones seem more efficient and realistic in real life. While UAVs are widely used in last-mile deliveries, they can also be used in wireless communication networks to fully display their benefits: flexibility, capability to optimize their locations in real time, and providing an additional capacity of the cellular networks.

APPENDIX
PROOF OF THEOREM 1

In this section, we provide the proof of the distribution of R_b. The same method as computing the first nearest neighbor in PPP, the probability of $R_b > r$ equals to the probability of no point falling in the certain area, say A

$$\mathbb{P}(R_b > r) = \mathbb{P}(\mathcal{N}(A) = 0) \tag{33}$$

where A is the shadowing area in Fig. 9. In this case, to compute the CDF of R_b, we need to compute the area of A.

To do so, we divide A into three subareas, as shown in Fig. 10. Observing that in the case of different relationships between θ and L_1, the area of A_1 and the equation of computing A_2 keep the same, while A_3 changes. Hence, we mainly focus on A_3.

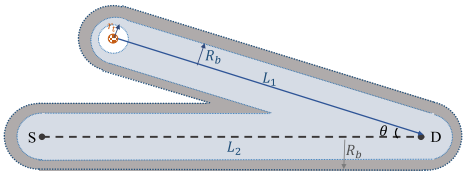

Fig. 9. Illustration of the distance distribution of R_b.

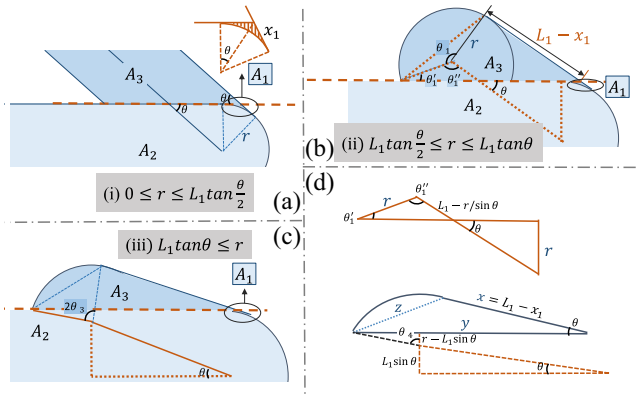

Fig. 10. Proof of counting the area for R_b.

As Fig. 10 shows, A_2 is consisted of a rectangle and two semicircles, thus the area is

$$|A_2| = L_2 \times 2R_b + 2 \times \frac{1}{2}\pi R_b^2 \tag{34}$$

while $|A_1|$ is computing by the triangle subtract the chord, and x_1 is simply given by the triangular relationship

$$\begin{aligned} |A_1| &= 2R_b \times x_1 - \frac{2\theta}{2\pi}\pi R_b^2, \\ x_1 &= R_b \tan(\theta). \end{aligned} \tag{35}$$

$|A_3|$ is slightly more complex compared with another two areas. We consider three possible cases as shown in Fig. 10(a)–(d) we plot two important geometry relationships of (b) and (c). The proof completes by using the counting measure of Poisson distribution

$$\mathbb{P}(R_b > r) = \mathbb{P}(\mathcal{N}(A) = 0) = \exp(-\lambda_b |A|). \tag{36}$$

REFERENCES

[1] S. Sekander, H. Tabassum, and E. Hossain, "Multi-tier drone architecture for 5G/B5G cellular networks: Challenges, trends, and prospects," *IEEE Commun. Mag.*, vol. 56, no. 3, pp. 96–103, Mar. 2018.

[2] M. Mozaffari, W. Saad, M. Bennis, Y.-H. Nam, and M. Debbah, "A tutorial on UAVs for wireless networks: Applications, challenges, and open problems," *IEEE Commun. Surveys Tuts.*, vol. 21, no. 3, pp. 2334–2360, 3rd Quart., 2019.

[3] B. Li, Z. Fei, and Y. Zhang, "UAV communications for 5G and beyond: Recent advances and future trends," *IEEE Internet Things J.*, vol. 6, no. 2, pp. 2241–2263, Apr. 2019.

[4] Y. Zeng, R. Zhang, and T. J. Lim, "Wireless communications with unmanned aerial vehicles: Opportunities and challenges," *IEEE Commun. Mag.*, vol. 54, no. 5, pp. 36–42, May 2016.

[5] M. Khosravi, S. Enayati, H. Saeedi, and H. Pishro-Nik, "Multi-purpose drones for coverage and transport applications," *IEEE Trans. Wireless Commun.*, vol. 20, no. 6, pp. 3974–3987, Jun. 2021.

[6] A. Al-Hourani, S. Kandeepan, and S. Lardner, "Optimal LAP altitude for maximum coverage," *IEEE Wireless Commun. Lett.*, vol. 3, no. 6, pp. 569–572, Dec. 2014.

[7] M. Alzenad and H. Yanikomeroglu, "Coverage and rate analysis for vertical heterogeneous networks (VHetNets)," *IEEE Trans. Wireless Commun.*, vol. 18, no. 12, pp. 5643–5657, Dec. 2019.

[8] N. H. Motlagh, T. Taleb, and O. Arouk, "Low-altitude unmanned aerial vehicles-based Internet of Things services: Comprehensive survey and future perspectives," *IEEE Internet Things J.*, vol. 3, no. 6, pp. 899–922, Dec. 2016.

[9] A. K. Gupta, S. Ghosh, and M. R. Bhatnagar, "Pricing scheme for UAV-enabled charging of sensor network," in *Proc. IEEE 18th India Council Int. Conf. (INDICON)*, 2021, pp. 1–6.

[10] N. Naren et al., "IoMT and DNN-enabled drone-assisted COVID-19 screening and detection framework for rural areas," *IEEE Internet Things Mag.*, vol. 4, no. 2, pp. 4–9, Jun. 2021.

[11] A. Otto, N. Agatz, J. Campbell, B. Golden, and E. Pesch, "Optimization approaches for civil applications of unmanned aerial vehicles (UAVs) or aerial drones: A survey," *Networks*, vol. 72, no. 4, pp. 411–458, 2018.

[12] S. R. R. Singireddy and T. U. Daim, "Technology roadmap: Drone delivery–Amazon prime air," in *Infrastructure and Technology Management*. Heidelberg, Germany: Springer, 2018, pp. 387–412.

[13] A. Welch, "A cost-benefit analysis of Amazon prime air," M.S. thesis, Dept. Economics, Univ. Tennessee Chattanooga, Chattanooga, TN, USA, 2015.

[14] W. Yoo, E. Yu, and J. Jung, "Drone delivery: Factors affecting the public's attitude and intention to adopt," *Telematics Inf.*, vol. 35, no. 6, pp. 1687–1700, 2018.

[15] N. Agatz, P. Bouman, and M. Schmidt, "Optimization approaches for the traveling salesman problem with drone," *Transp. Sci.*, vol. 52, no. 4, pp. 965–981, 2018.

[16] G. Ling and N. Draghic, "Aerial drones for blood delivery," *Transfusion*, vol. 59, no. S2, pp. 1608–1611, 2019.

[17] E. Ackerman and M. Koziol, "The blood is here: Zipline's medical delivery drones are changing the game in rwanda," *IEEE Spectr.*, vol. 56, no. 5, pp. 24–31, May 2019.

[18] A. Kumar, K. Sharma, H. Singh, S. G. Naugriya, S. S. Gill, and R. Buyya, "A drone-based networked system and methods for combating coronavirus disease (COVID-19) pandemic," *Future Gener. Comput. Syst.*, vol. 115, pp. 1–19, Feb. 2021.

[19] B. Rabta, C. Wankmüller, and G. Reiner, "A drone fleet model for last-mile distribution in disaster relief operations," *Int. J. Disaster Risk Reduction*, vol. 28, pp. 107–112, Jun. 2018.

[20] S. Poikonen, X. Wang, and B. Golden, "The vehicle routing problem with drones: Extended models and connections," *Networks*, vol. 70, no. 1, pp. 34–43, 2017.

[21] A. Nedjati, B. Vizvari, and G. Izbirak, "Post-earthquake response by small UAV helicopters," *Nat. Hazards*, vol. 80, no. 3, pp. 1669–1688, 2016.

[22] G. Zhu and P. Wei, "Pre-departure planning for urban air mobility flights with dynamic airspace reservation," in *Proc. AIAA Aviation Forum*, 2019, p. 3519.

[23] M. Samir, S. Sharafeddine, C. M. Assi, T. M. Nguyen, and A. Ghrayeb, "UAV trajectory planning for data collection from time-constrained IoT devices," *IEEE Trans. Wireless Commun.*, vol. 19, no. 1, pp. 34–46, Jan. 2020.

[24] Q. Zhang, M. Jiang, Z. Feng, W. Li, W. Zhang, and M. Pan, "IoT enabled UAV: Network architecture and routing algorithm," *IEEE Internet Things J.*, vol. 6, no. 2, pp. 3727–3742, Apr. 2019.

[25] M. Mozaffari, W. Saad, M. Bennis, and M. Debbah, "Mobile unmanned aerial vehicles (UAVs) for energy-efficient Internet of Things communications," *IEEE Trans. Wireless Commun.*, vol. 16, no. 11, pp. 7574–7589, Nov. 2017.

[26] L. Xie, J. Xu, and R. Zhang, "Throughput maximization for UAV-enabled wireless powered communication networks," *IEEE Internet Things J.*, vol. 6, no. 2, pp. 1690–1703, Apr. 2019.

[27] M. Mozaffari, W. Saad, M. Bennis, and M. Debbah, "Efficient deployment of multiple unmanned aerial vehicles for optimal wireless coverage," *IEEE Commun. Lett.*, vol. 20, no. 8, pp. 1647–1650, Aug. 2016.

[28] H. Menouar, I. Guvenc, K. Akkaya, A. S. Uluagac, A. Kadri, and A. Tuncer, "UAV-enabled intelligent transportation systems for the smart city: Applications and challenges," *IEEE Commun. Mag.*, vol. 55, no. 3, pp. 22–28, Mar. 2017.

[29] Z. Chen, K. Chi, K. Zheng, G. Dai, and Q. Shao, "Minimization of transmission completion time in UAV-enabled wireless powered communication networks," *IEEE Internet Things J.*, vol. 7, no. 2, pp. 1245–1259, Feb. 2020.

[30] Y. Qin, M. A. Kishk, and M.-S. Alouini. "Energy efficiency analysis of charging PADs-powered UAV-enabled wireless networks." 2022. [Online]. Available: https://arxiv.org/abs/2208.03649

[31] Y. Zhou et al., "Secure communications for UAV-enabled mobile edge computing systems," *IEEE Trans. Commun.*, vol. 68, no. 1, pp. 376–388, Jan. 2020.
[32] R. Amer, W. Saad, and N. Marchetti, "Mobility in the sky: Performance and mobility analysis for cellular-connected UAVs," *IEEE Trans. Commun.*, vol. 68, no. 5, pp. 3229–3246, May 2020.
[33] H. ElSawy, A. Sultan-Salem, M.-S. Alouini, and M. Z. Win, "Modeling and analysis of cellular networks using stochastic geometry: A tutorial," *IEEE Commun. Surveys Tuts.*, vol. 19, no. 1, pp. 167–203, 1st Quart., 2017.
[34] H. ElSawy, E. Hossain, and M. Haenggi, "Stochastic geometry for modeling, analysis, and design of multi-tier and cognitive cellular wireless networks: A survey," *IEEE Commun. Surveys Tuts.*, vol. 15, no. 3, pp. 996–1019, 3rd Quart., 2013.
[35] G. Hattab and D. Cabric, "Energy-efficient massive IoT shared spectrum access over UAV-enabled cellular networks," *IEEE Trans. Commun.*, vol. 68, no. 9, pp. 5633–5648, Sep. 2020.
[36] B. Galkin, J. Kibilda, and L. A. DaSilva, "A stochastic model for UAV networks positioned above demand hotspots in urban environments," *IEEE Trans. Veh. Technol.*, vol. 68, no. 7, pp. 6985–6996, Jul. 2019.
[37] M. Alzenad, A. El-Keyi, and H. Yanikomeroglu, "3-D placement of an unmanned aerial vehicle base station for maximum coverage of users with different QoS requirements," *IEEE Wireless Commun. Lett.*, vol. 7, no. 1, pp. 38–41, Feb. 2018.
[38] C. Saha, M. Afshang, and H. S. Dhillon, "Enriched K-tier HetNet model to enable the analysis of user-centric small cell deployments," *IEEE Trans. Wireless Commun.*, vol. 16, no. 3, pp. 1593–1608, Mar. 2017.
[39] Y. Qin, M. A. Kishk, and M.-S. Alouini, "Drone charging stations deployment in rural areas for better wireless coverage: Challenges and solutions," *IEEE Internet Things Mag.*, vol. 5, no. 1, pp. 148–153, Mar. 2022.
[40] Y. Qin, M. A. Kishk, and M.-S. Alouini, "On the influence of charging stations spatial distribution on aerial wireless networks," *IEEE Trans. Green Commun. Netw.*, vol. 5, no. 3, pp. 1395–1409, Sep. 2021.
[41] Y. Qin, M. A. Kishk, and M.-S. Alouini, "Performance evaluation of UAV-enabled cellular networks with battery-limited drones," *IEEE Commun. Lett.*, vol. 24, no. 12, pp. 2664–2668, Dec. 2020.
[42] S. Enayati, H. Saeedi, H. Pishro-Nik, and H. Yanikomeroglu, "Moving aerial base station networks: A stochastic geometry analysis and design perspective," *IEEE Trans. Wireless Commun.*, vol. 18, no. 6, pp. 2977–2988, Jun. 2019.
[43] N. Senadhira, S. Durrani, X. Zhou, N. Yang, and M. Ding, "Uplink NOMA for cellular-connected UAV: Impact of UAV trajectories and altitude," *IEEE Trans. Commun.*, vol. 68, no. 8, pp. 5242–5258, Aug. 2020.
[44] M. Banagar and H. S. Dhillon, "3GPP-inspired stochastic geometry-based mobility model for a drone cellular network," in *Proc. IEEE Global Commun. Conf. (GLOBECOM)*, 2019, pp. 1–6.
[45] Y. Zeng, J. Xu, and R. Zhang, "Energy minimization for wireless communication with rotary-wing UAV," *IEEE Trans. Wireless Commun.*, vol. 18, no. 4, pp. 2329–2345, Apr. 2019.

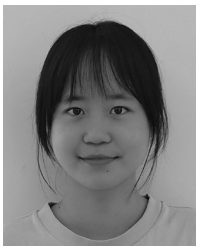

Yujie Qin received the B.Sc. degree from the University of Science and Technology of China, Hefei, China, in 2020, and the M.Sc. degree from the King Abdullah University of Science and Technology, Thuwal, Saudi Arabia, in 2021, where she is currently pursuing the Ph.D. degree with the Communication Theory Lab.

Her current research interests include stochastic geometry and UAV communication.

Mustafa A. Kishk (Member, IEEE) received the B.Sc. and M.Sc. degrees in electrical engineering from Cairo University, Giza, Egypt, in 2013 and 2015, respectively, and the Ph.D. degree in electrical engineering from Virginia Tech, Blacksburg, VA, USA, in 2018.

He is an Assistant Professor with the Electronic Engineering Department, Maynooth University, Maynooth, Ireland. Before that, he was a Postdoctoral Research Fellow with the Communication Theory Laboratory, King Abdullah University of Science and Technology, Thuwal, Saudi Arabia. His current research interests include stochastic geometry, energy harvesting wireless networks, UAV-enabled communication systems, and satellite communications.

Dr. Kishk currently serves as an Associate Editor for IEEE WIRELESS COMMUNICATION LETTERS.

Mohamed-Slim Alouini (Fellow, IEEE) was born in Tunis, Tunisia. He received the Ph.D. degree in electrical engineering from California Institute of Technology, Pasadena, CA, USA, in 1998.

He served as a Faculty Member with the University of Minnesota, Minneapolis, MN, USA, then with the Texas A&M University at Qatar, Doha, Qatar, before joining the King Abdullah University of Science and Technology, Thuwal, Makkah Province, Saudi Arabia, as a Professor of Electrical Engineering in 2009. His current research interests include the modeling, design, and performance analysis of wireless communication systems.